CrossMark

ORIGINAL PAPER

Analysis of static bending-induced compression wood formation in juvenile *Picea omorika* (Pančić) Purkyně

Aleksandra Mitrović[1] · Lloyd A. Donaldson[2] · Daniela Djikanović[1] ·
Jelena Bogdanović Pristov[1] · Jasna Simonović[1] · Dragosav Mutavdžić[1] ·
Aleksandar Kalauzi[1] · Vuk Maksimović[1] · Bernadette Nanayakkara[2] ·
Ksenija Radotić[1]

Abstract

Key message **Young *P. omorika* trees subjected to static bending showed a severe compression wood response as characterized by fluorescence spectroscopy/microscopy, which decreased in severity with height correlated with a decrease in bending moment.**

Abstract This investigation is aimed at understanding the reaction wood response in a slow-growing conifer species under conditions of severe and long-term bending stress. Compression wood (CW) formation was studied in stems of juvenile *P. omorika* after trees were subjected to static bending by wiring at an angle of about 90 degrees, for 1 year. The applied static bending would correspond to the impact of winter snow loads or snow falls on juvenile conifers. Stem sections were collected during one growing season and examined by fluorescence microscopy, and fluorescence spectroscopy including deconvolution analysis. Trees exposed to bending produced large amounts of severe CW but very low amounts of opposite wood (OW) during the experimental season indicating a dramatic change in biomass distribution compared to control trees. Indicators of cell wall structure changes, such as fluorescence emission spectra, peak intensities, and shifts in the positions of the long-wavelength spectral components, decreased from the stem base to the top of the stem, in line with a calculated decrease in bending moment.

Communicated by T. Fourcaud.

✉ Ksenija Radotić
xenia@imsi.rs

[1] Institute for Multidisciplinary Research, University of Belgrade, Kneza Viseslava 1, 11000 Belgrade, Serbia

[2] Scion, Private Bag 3020, Rotorua, New Zealand

Abbreviations
APD Approximation of the probability density
CW   Compression wood
FAA Formalin aceto-alcohol
OW   Opposite wood

Introduction

Picea omorika (Pančić) Purkyně is a slow-growing Balkan endemic coniferous species and Tertiary relict of the European flora with a natural habitat reduced to the middle and upper courses of the Drina river. Despite its limited natural range, *P. omorika* is considered to be one of the most adaptable spruces.

Formation of reaction wood in the stem is a response to leaning as part of the gravitropic response of the tree. In conifers, reaction wood is known as compression wood (CW). Its formation occurs on the lower side of the leaning stem, resulting in eccentric growth (Timell 1986; Donaldson and Singh 2013). Wood opposite to the compression wood in the same growth ring is termed opposite wood (OW), while wood from growth rings that do not contain any CW is termed normal wood (Timell 1986; Donaldson and Singh 2013). CW occurs in a range of gradations from near normal wood to severe CW, mild CW forming a continuum between normal wood and severe CW. In slow-growing conifer species, CW typically occurs in a severe form, but in fast-growing species and in juvenile wood, a

Springer

mild form of CW is mostly present, with properties intermediate between normal wood and severe CW (Donaldson et al. 2004; Nanayakkara et al. 2014). CW is characterized by both increased wall thickness and reduced lumen diameter compared to normal wood (Donaldson et al. 2004). In CW, the angle of the cellulose microfibrils in the S2 layer of the cell wall is higher than in normal wood, tracheid length is reduced, cell cross-sectional profile is rounder, and there are often intercellular spaces at the cell corners (Donaldson and Singh 2013).

Compression wood is highly lignified, and consequently contains less cellulose than normal wood. Reduced lignification of the middle lamella is the earliest detectable sign of CW formation and the extent of increased secondary wall lignification is the most reliable marker for CW severity (Donaldson et al. 2004). The composition of lignin is also changed in CW, with increased amounts of *p*-hydroxyphenyl monomers and increased condensation of monomer units in the polymer (Fukushima and Terashima 1991; Timell 1986). Compression wood contains greatly increased amounts of galactan, and slightly lower amounts of mannan and xylan compared to normal wood (Nanayakkara et al. 2009; Donaldson and Knox 2012; Donaldson and Singh 2013).

Autofluorescence of wood and pulp is considered to originate mainly from lignin (Castellan and Davidson 1994; Olmstead and Gray 1997; Albinsson et al. 1999), and certain chemical groups have been identified, including coniferyl alcohol, biphenyl, phenylcoumarane and stilbene as the likely components responsible for fluorescence (Falkehag et al. 1966; Konschin and Sundholm 1974; Lundquist et al. 1978).

Most literature data concerning CW formation have been obtained from experiments using stem tilting or leaning. Only a few studies deal with reaction of conifers to severe bending stress (Sinott 1952; Downes et al. 1994). Our investigation is aimed at understanding the reaction wood response in a slow-growing conifer species under conditions of severe and constant (long-term) bending stress. We studied CW formation in stems of juvenile *P. omorika* trees that were subjected to static bending by wiring at an angle of about 90 degrees, for 1 year. *P. omorika* in its natural habitats (cliffs, forest clearings) survives under the influence of extreme mechanical forces—strong northerly wind, snow and rockfalls. The applied static bending would correspond to the impact of winter snow loads or snow falls on juvenile conifers. We investigated structural parameters that can reveal fine cell wall modifications along the stem, by recording the fluorescence properties of CW and OW of *P. omorika* stem sections by high-resolution spectral confocal microscopy and corresponding spectral deconvolution. By deconvolution of the emission spectra, we compared the number and nature of spectral components in compression and opposite wood, related to fluorophores/structural units in these two wood types. This allows structural interpretation of the response to mechanical stress in *P. omorika* juvenile trees.

Experimental methods

Plant material and sample collection

Four-year-old *P. omorika* plants about 70 cm tall were grown in plastic pots ($20 \times 20 \times 20$ cm) outdoors in Belgrade, Serbia (44°49′N, 20°29′E). Static bending stress was applied at the end of the growing season, in October 2009. Bending was performed at 37 cm from the stem base by wiring (the bending angle was about 90 degrees). The same bending force among 40 plants subjected to bending was provided using wire of the same length and fixing it to the edge of each pot (Fig. 1a). As a control, 40 plants of the same age were used, grown under the same conditions as bent plants but without any bending treatment.

Stem samples (about 3 cm long) were taken on the day wiring was performed (on October 23, 2009—control plants), during the winter season (2 months after wiring, on December 25, 2009), in spring (6 months after wiring, on April 28, 2010), during summer (9 months after wiring, on July 22, 2010) and 1 year after wiring (on October 25, 2010). Stem samples were collected from wired plants at about 10, 20 and 30 cm from the stem base, while in control plants a single collection was made at about 10 cm from the stem base. All stem samples were debarked and fixed in formalin aceto-alcohol (FAA).

Stem height and stem diameter at 10, 20 and 30 cm from the stem base in control and bent plants were measured before sample collection (for each of 5 time points, 8 controls and 8 bent plants were measured). The amounts of compression and opposite wood formed during the experiment were measured by counting the number of tracheids in the current growth ring and by measuring growth ring width on both sides of the stem.

Bending moment calculation

To quantify the applied mechanical force, the bending moment caused by wiring of *P. omorika* plants was calculated. A set of weights was used to cause the same stem bending as in wired plants, and the X and Y components of points 10 cm, 20 cm, 30 and 37 cm from the base of the stem, the length of wire fixed on 37 cm from the base of the stem and on the pot edge, and the distance from stem base to the pot edge, were measured (Fig. 1c). In eight *P. omorika* plants at 37 cm from the base of the stem, weights necessary to bend the *P. omorika* stem to the same extent

Fig. 1 Juvenile *P. omorika* trees: **a** wired plant at the beginning of the experiment in October 2009; **b** tree untied after the end of experiment in December 2010 with visible second curvature (with the start of vegetation period 2010 trees subjected to static bending produced a second curvature uprighting the apex); **c** bending moment calculation for the *P. omorika* tree bent by wiring. $M_{10, 20, 30}$ = bending moment at 10, 20, 30 cm from stem base; G = Earth's gravity force
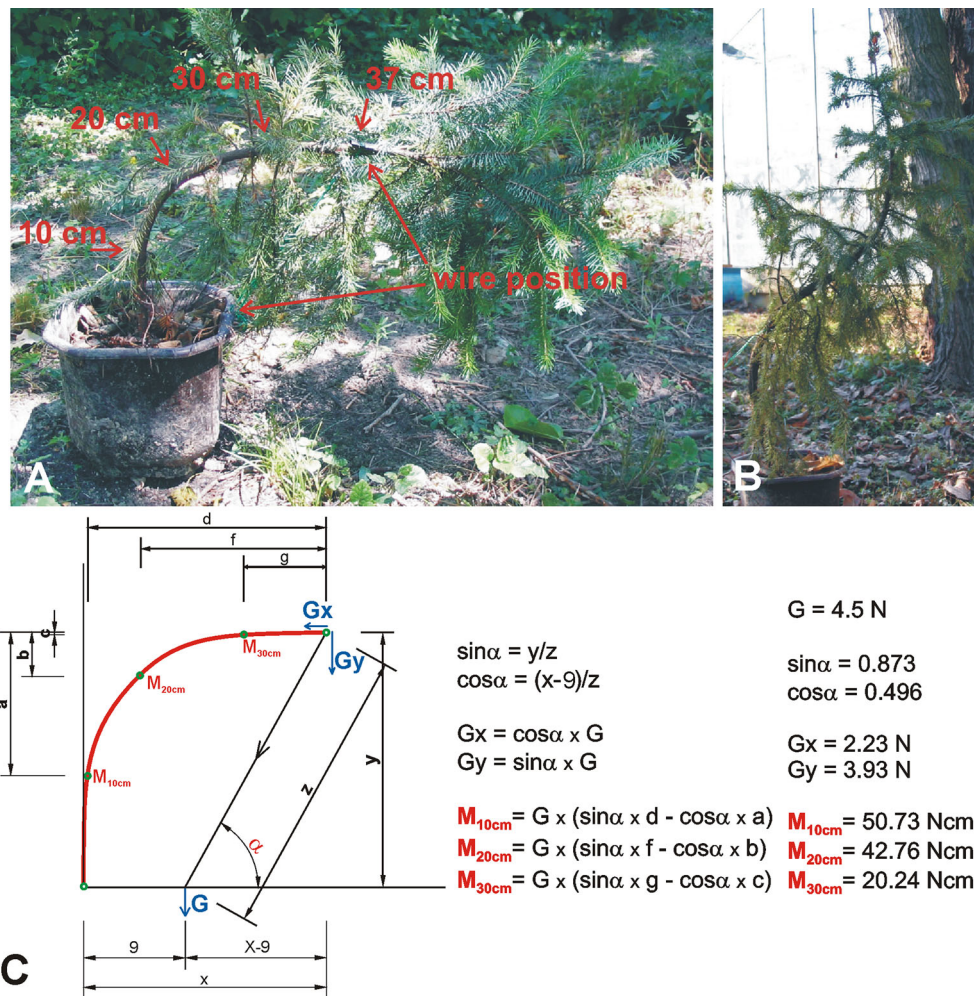
as in the wired plants were hung on the wire pulled through the hole on the edge of the pot (the same hole used for fixing the wire in wired plants). The average weight required to bend the stem was 458 ± 12 g.

Immunocytochemistry

Transverse sections from fixed stem samples 60 μm in thickness were treated with a 1:20 dilution of LM5 primary rat monoclonal antibody in 0.01 M phosphate-buffered saline containing 1 % (w/v) acetylated bovine serum albumin as a blocking agent and 5 mM sodium azide (Jones et al. 1997) for 2 h at room temperature. After washing in phosphate-buffered saline, sections were treated with Goat anti-Rat secondary antibody labeled with Alexa 568 (Invitrogen) for 2 h at room temperature followed by further washing. Sections were mounted in 50 % glycerol at pH7 (Donaldson 2013) and examined by confocal fluorescence microscopy with sequential excitation at 488 and 561 nm. Control sections were treated only with the secondary antibody and imaged under identical conditions.

Fluorescence confocal imaging, spectral acquisition and deconvolution

Fixed stem samples (stem segments from 1 control and 1 bent plant from each time point) were sectioned at 60 μm thickness in the transverse plane using a sledge microtome. Sections were mounted in 50 % glycerol at pH 9 (Donaldson 2013) and imaged using a Leica SP5 II confocal microscope. Spectral sequences were acquired using 355 nm excitation at 5 nm intervals with a 10 nm slit width from 400 to 700 nm. For each sample examined, spectral sequences were acquired at two locations in CW and in OW of the same or previous growth ring. Control plants contained compression wood despite the lack of bending treatment. At each of the two locations, five spectra were measured in smaller regions of interest giving a total of ten spectra per sample for both OW and CW. Spectra were measured from the spectral image sequence by measuring the average brightness of objects (cell walls) using a threshold of 10 gray levels to exclude empty background regions in the lumens of cells.

Each of the ten spectra per sample was deconvolved into two log–normal components using the log–normal method (Radotić et al. 2006; Kalauzi et al. 2007). Non-linear fitting of all fluorescence spectra was performed using the Nelder–Mead simplex algorithm implemented in Matlab 6.5. As a result of the non-linear fitting, the total number of components was obtained for each wood type. Positions of all components were treated as a random variable so that histograms of component positions were calculated. Since histogram profiles (positions and relative amplitudes of histogram maxima) depended on the number of histogram abscissa intervals, a series of histograms was constructed with an increasing number of abscissa intervals. An approximation of the probability density (APD) for a component to assume a position on the wavelength axis could then be reconstructed by weighed averaging of histogram values for a set of histograms.

Data analysis

Analysis of variance (two- or three-way Anova, depending on number of factors) at $P < 0.05$ was used for estimation of differences in growth parameters of wood samples.

Results and discussion

Growth parameters and wood imaging

Static bending by wiring in juvenile *P. omorika* trees (Fig. 1a) was performed at the end of the growth period in autumn 2009, so CW formation as a result of static bending occurred at the beginning of the next growth period in April 2010. Stem height growth was decreased, while diameter growth was increased in bent plants compared to controls (Fig. 2a, b). Stem diameter did not vary considerably along the stem (at 10, 20, 30 cm from stem base) in both control and bent plants. Mechanical perturbations such as flexing have been shown to increase radial growth and reduce stem elongation (Telewski and Jaffe 1986; Telewski and Pruyn 1998; Kern et al. 2005). Similar effects have been described for tilting experiments associated with compression wood formation (Lachenbruch et al. 2010; Nanayakkara et al. 2014). Figure 3 shows images of *P. omorika* stem cross sections from a control plant and a plant exposed to static bending after 1 year. It is interesting to note that in the base stem segment (10 cm position) of the treated plants, CW formed on one side of the stem was very thick, but on the opposite side there was almost no wood formation (<5 tracheids), indicating that the tree had put all of its resources into making CW. The amount of CW and OW formed during the experimental periods was
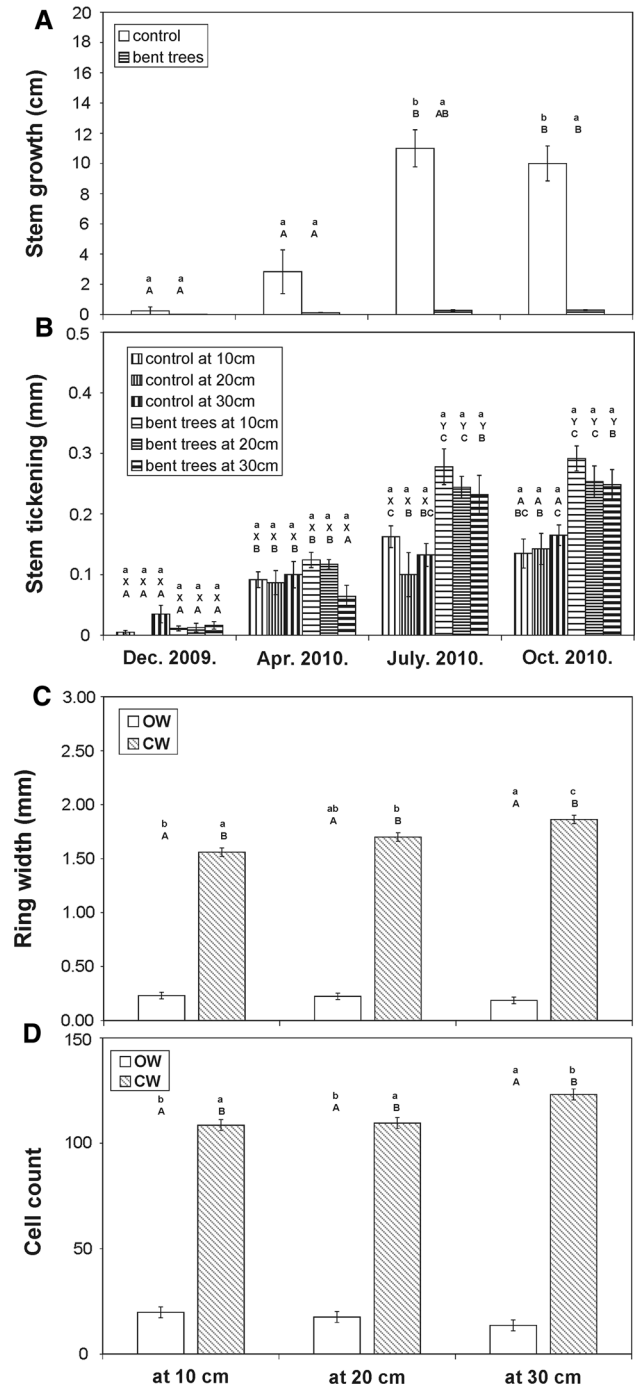

Fig. 2 Growth parameters in stem segments of control and mechanically treated juvenile *Picea omorika*; **a** stem growth; **b** stem thickening; **c** forming ring width on the compression and opposite side, July 2010 bent tree; **d** number of cells on the compression and opposite side of the forming ring, July 2010 bent tree; *OW* opposite wood, *CW* compression wood; mean ± SE; $n = 8$; *Asterisk* significant difference at $P < 0.05$ against control from October 2009; *A, B, C* significant difference at $P < 0.05$ among seasons; *a, b* significant difference at $P < 0.05$ among stem segments within a season; *X, Y* significant difference at $P < 0.05$ against matching segment in control tree within each season; mean values marked with *different letters* are significantly different

Fig. 3 Images of the *P. omorika* stem cross section, from **a** base stem segment of *P. omorika* tree exposed to static bending, after 1 year and **b** control plant. The control plant contains small scattered areas of compression wood, while the plant exposed to static bending has a large area of compression wood on the *lower* side of the stem (*C*), while there was almost no wood formation (<5 tracheids) on the *opposite* side (*O*) of the stem. Scale bar = 2 mm
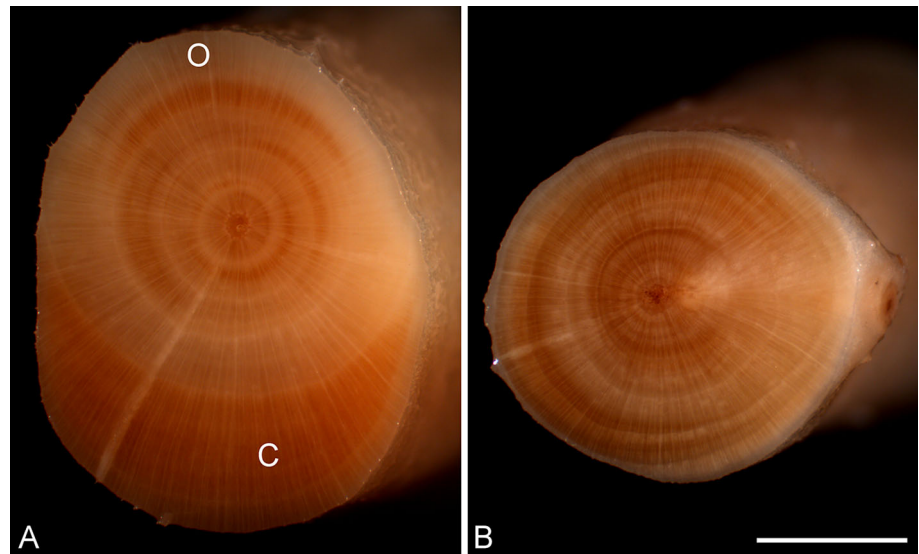
Fig. 4 Confocal fluorescence images (excitation 488 and 561 nm) that correspond to the optical images from Fig. 3, showing a section through the growth rings of the October 2010 samples of *P. omorika* experimental and control trees. **a** *Compression* wood (*CW*) formed during the bending experiment. **b** *Opposite* wood (*OW*). **c** Wood formed by the control trees. **a** and **b**, Scale bar = 500 μm. **c**, Scale bar 250 μm
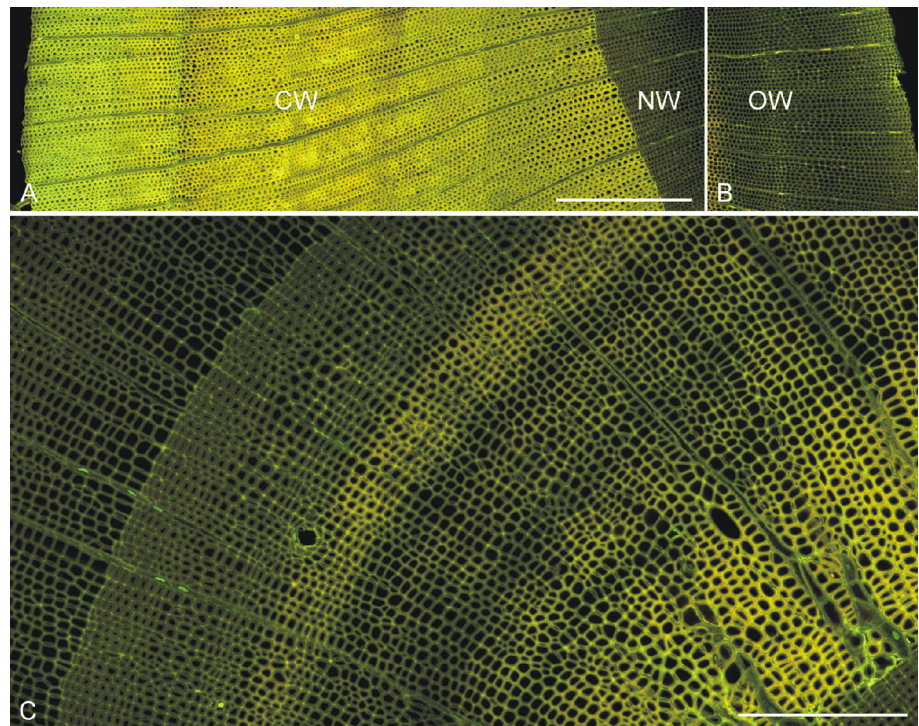

observed by both measurements of the width and cell counting (Fig. 2c, d). In the samples collected in July 2010, the amount of CW increased from the base of the stem to the 30 cm position, while the amount of OW did not vary significantly. Compression wood formation based on cell counts from the start of earlywood to the last fully differentiated tracheid was about five times the amount of OW at the base of the bent stem increasing to nine times the amount of OW at the 30 cm position. A similar trend was observed in the April and October 2010 samples. Based on the literature (Lachenbruch et al. 2010; Nanayakkara et al.

2014), a greater amount of compression wood is expected in the stem as a response to leaning at the base of the stem compared to positions closer to the top. However, with the start of the growth period (in April 2010) in *P. omorika* juvenile trees subjected to static bending, the overcorrection bending of the stem occurred below the apex (Fig. 1b). This overcorrection growth in juvenile conifers is common in gravitropic studies (Sinott 1952; Downes et al. 1994). Hence, at 30 cm from stem base, the amount of CW produced was the cumulative response to both static bending that we implemented and overcorrection growth.

The confocal fluorescence images corresponding to Fig. 3 are presented in Fig. 4. Compression and normal wood in the treated trees and in the control trees can be distinguished by the difference in brightness in these visible excitation images. The CW is much brighter than the OW, and this difference is more pronounced in the bent than in the control trees indicating a much higher degree of CW severity (Donaldson et al. 2004). Wood formed by the control trees consists of normal wood mixed with various
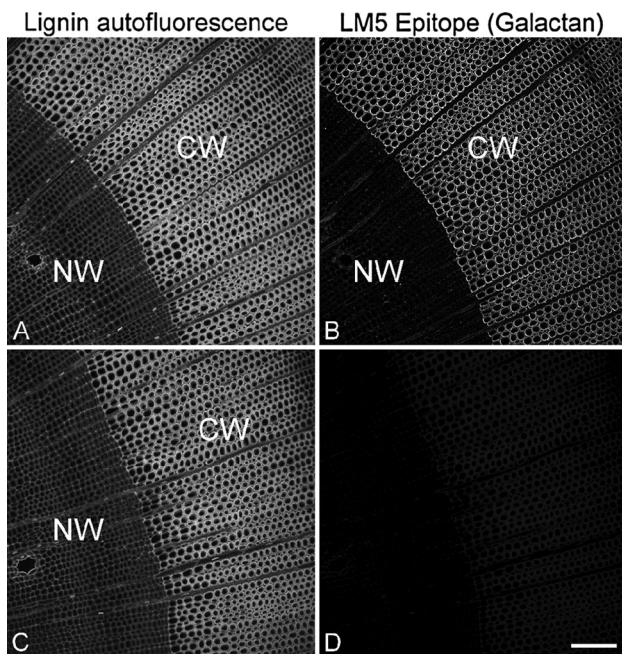
Fig. 5 Confocal fluorescence images of lignin autofluorescence at 488 nm excitation and immunolocalised galactan (LM5 epitope) labeled with a secondary antibody conjugated to Alexa 568 at 561 nm excitation. **a** Lignin autofluorescence in normal (*NW*) and compression wood (*CW*) formed during the bending experiment. **b** Galactan distribution localized almost entirely to the compression wood. **c** Lignin autofluorescence in normal and compression wood in the absence of primary antibody to galactan. **d** A control image showing weak lignin autofluorescence at 561 nm excitation in the absence of primary antibody to galactan and at the same exposure as **b**. *Scale bar* 110 µm
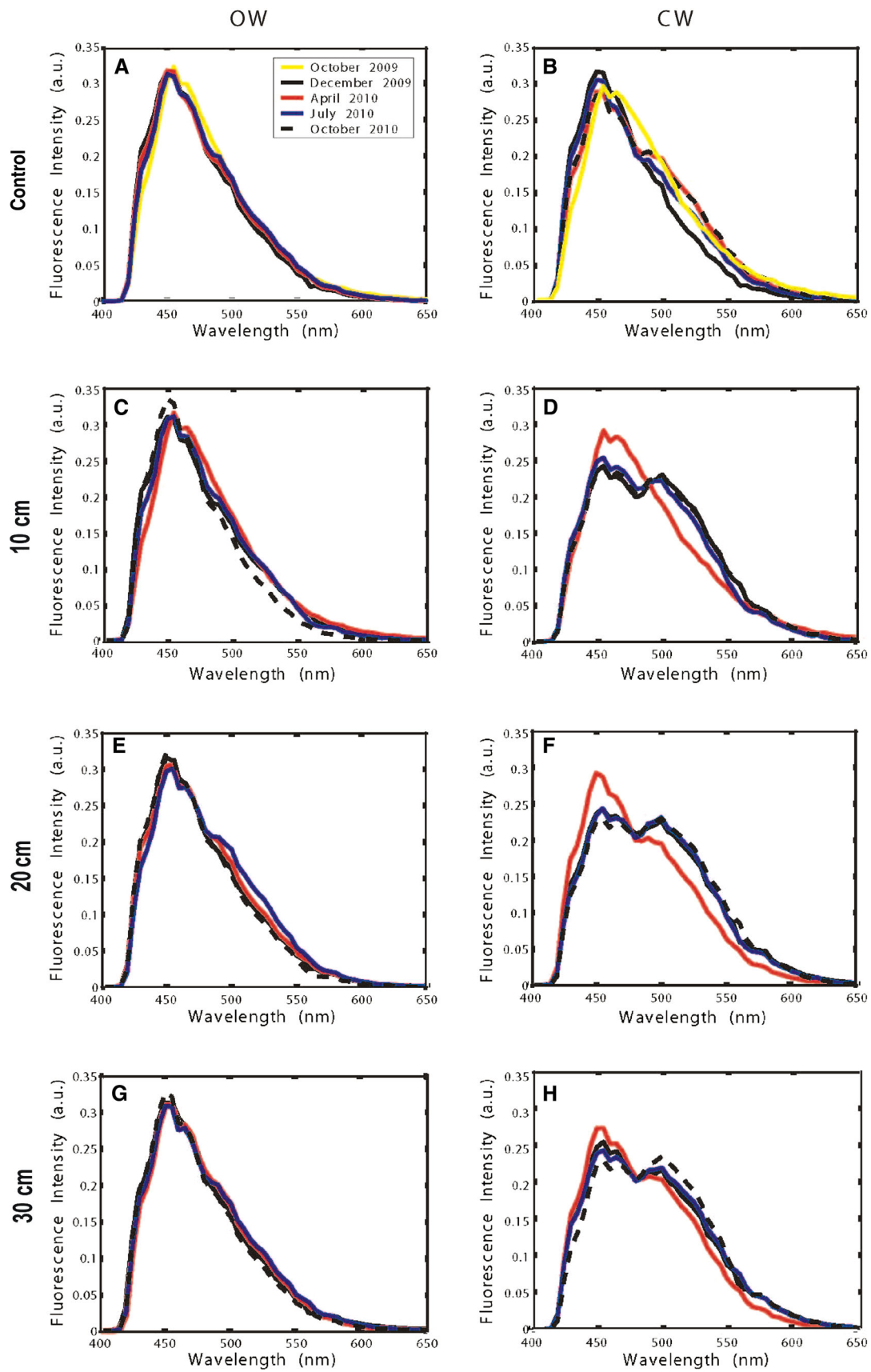
Fig. 6 Emission spectra of compression wood (*right column* **b, d, f, ▶ h**) and corresponding opposite wood (*left column* **a, c, e, g**) from the same growth ring, for the control plant and for the stem segments (10, 20 and 30 cm from the base of the stem) in the treated plant; the control plant contained compression wood despite the lack of bending treatment; *a.u* arbitrary units

types of compression wood from mild to more severe grades as shown by bands of varying brightness. This difference in brightness is due both to the increased amount of lignin and the increased quantum yield of the lignin fluorescence which presumably results from unknown molecular changes, possibly including the increased content of *p*-hydroxyphenyl lignin (Donaldson et al. 2010).

Fluorescence spectroscopy

Fluorescence emission spectra from the outer part of the developing growth ring in segments of control and treated trees sampled at different seasons during 1 year are characterized by an integral emission spectrum with three distinguished peaks, at 455 (the main lignin peak), 470 and 510 nm (Fig. 6).

Since in the base stem segments the OW from the same growth ring was very thin, spectral comparisons were made using normal wood from the previous growth ring. As lignification of latewood tracheids is often incomplete at the onset of winter and completes with early spring (Donaldson 1992), completion of lignification of the outer part of previous growth ring may have occurred concurrently with the performed static bending. In OW of both control and treated plants, two peaks, at 455 nm and 470 nm, are visible, regardless of season during the year. The peak at 470 nm decreases in OW from the base (Fig. 6c) to the top of the stem (Fig. 6g) (parallel to the decrease in bending moment, Fig. 1c), being least expressed in OW of control plants (Fig. 6a), regardless of season during the year. The peak at 510 nm is poorly expressed in OW and, similar to the 470 peak, there is a trend of

Table 1 Band shifts/differences of corresponding APD components (I and II) positions between compression (CW) and opposite (OW) wood, for controls and stem segments of bent trees at 10, 20 and 30 cm from stem base, at the dates of sample collection

Component Band shift (nm)	October 2009		December 2009		April 2010		July 2010		October 2010	
	I (CW-OW)	II (CW-OW)	I (CW-OW)	II (CW-OW)	I (CW-OW)	II (CW-OW)	I (CW-OW)	II (CW-OW)	I (CW-OW)	II (CW-OW)
Control	1	−6.56	4.1	23.35	2.1	7.78	−3.3	2.95	−0.7	1.48
10 cm	–	–	7	13.3	2.5	11.32	0.9	3.81	6.9	19.1
20 cm	–	–	3.8	5.51	3.7	15.83	2.2	3.03	3.2	9.21
30 cm	–	–	2.1	1.76	−0.47	2.64	1.8	6.42	6.8	6.56

I and II are the two APD components (Figs. 7, 8) obtained by analysis of the corresponding emission spectra of the samples (Fig. 6)

decrease from the base (Fig. 6c) to the top of the stem (Fig. 6g) being least expressed in OW of control plants.

In CW, from the top to the base of the stem (Fig. 6d, f, h), an apparent increase in the intensity of peaks at 470 and 510 nm is visible, being least expressed in CW of control plants (Fig. 6b) regardless of season.

The absence of a 510 nm peak is characteristic of both OW and CW spectra from the October 2009 samples of the control tree (Fig. 6a, b) and the April 2010 base stem segment of the bent tree (Fig. 6c, d). As a characteristic of spectra from both OW and CW, this suggests that the absence of 510 nm peak is determined by a factor other than CW or OW lignin structure specificity.

In the April base stem segment from the wired tree (Fig. 6d), the absence of a 510 nm peak from the spectra of CW and its appearance and increase in segments at 20 cm (Fig. 6f) and 30 cm from the stem base (Fig. 6h) may be influenced by both the onset of the growth period and lignin deposition, being in accordance with bending severity. Fukushima and Terashima (1991) showed that in *Pinus thunbergii* CW, lignification of the middle lamella occurs at an earlier stage, with a considerable delay of the secondary wall lignification.

In the spectrum of CW of the April base segment of the treated tree (Fig. 6d), a shoulder at about 530 nm is visible. Its absence in other seasons and in upper stem segments (Fig. 6f, h) indicates a rigid molecular structure, formed with the onset of the growth period as a response to the highest bending moment (Fig. 1c) to which the base stem segment is exposed.

Spectral analysis

A characteristic of lignin fluorescence is that the emission spectrum contains multiple log–normal components originating from different fluorophores in the lignin molecule—shorter wavelengths corresponding to phenolic structures and longer wavelengths to conjugated structures. Deconvolution analysis allows us to characterize the number and location of component peaks by calculation of the approximation of the probability density (APD) of component positions. The positions of the spectral components obtained by this analysis (expressed as the APD maxima) are sensitive to the changes in lignin environments between normal and compression wood (Donaldson et al. 2010). Figure 7 shows the overlaid APD of component positions obtained by deconvolution of the 355 nm—excited emission spectra shown in Fig. 6. The two-component analysis of fluorescence spectra is useful to highlight the two main peaks in the integral spectra (Fig. 6), that is to highlight the main differences between *P. omorika* CW and OW in controls and trees exposed to static bending, in different growing seasons during 1 year. The analysis of the wood

Fig. 7 The overlaid approximate probability densities (APDs) of ▶ component positions obtained by deconvolution of 355 nm—excited emission spectra of the opposite (*left column* **a**, **c**, **e**, **g**) and compression wood (*right column* **b**, **d**, **f**, **h**), in control plants and in the plants exposed to static bending, for the sections at 10, 20 and 30 cm from the base of the stem

emission spectra shows variations in lignin structure which provide an estimate of compression wood severity.

The APDs (Fig. 7) of all samples contain the two maxima. In the APDs of both OW and CW spectra of October 2009 samples of the control tree (Fig. 6a, b), and the April 2010 base stem segment of the bent tree (Fig. 6c, d), characterized by the absence of a 510 nm peak, the two APD components approximate the two close peaks at 455 and 470 nm of the integral spectra (Fig. 6). The APD component that corresponds to the 470 nm peak of the integral spectra is absent in all other samples and is replaced by the component that corresponds to the 510 nm peak of the integral spectra (Figs. 6a–h, 7a–h).

The two-component APD analysis (Fig. 7) highlights, on one hand, the similarity of CW lignin structures among different samples (the overlay of both APD components) regardless of distance from stem base (i.e., bending moment) or season of tracheid maturation, and on the other, heterogeneity of lignin structures in OW (red shifts of both APD components). In OW, the shifts in the position of the long-wavelength APD component through seasons (Fig. 7) indicate variations in length of the rigid lignin chain structures induced by bending. These variations also increased from the top to the base of the stems, with the increase in bending moment (Fig. 1c).

The position of the emission maximum of a fluorophore may be significantly shifted as a result of perturbations in the fluorophore's microenvironments (Lakowicz 2006). Spectral differences observed between *P. omorika* CW and OW (Fig. 6) may be related to changes in lignin composition/structure or to changes in the composition and content of certain polysaccharides to which the lignin molecules are bound. It is known that in CW, β-1,4-galactan (absent in normal wood) is present in the outer secondary cell wall layer (Altaner et al. 2010; Donaldson and Knox 2012). Its quantity is regarded as one of the measures of compression severity (Nanayakkara et al. 2009). In stem samples of bent *P. omorika* trees, immunolocalisation using the LM5 antibody (Fig. 5) confirmed galactan localization exclusively in the CW. Also, CW lignin has greater *p*-hydroxyphenyl unit content compared to normal wood (Terashima and Fukushima 1988; Nanayakkara et al. 2009). Previous studies indicated that conjugated polymeric (lignin) structures (domains) containing guaiacyl and *p*-hydroxyphenyl units or their derivatives may form an extended framework of alternating C–C and C=C bonds. Such structures may be responsible
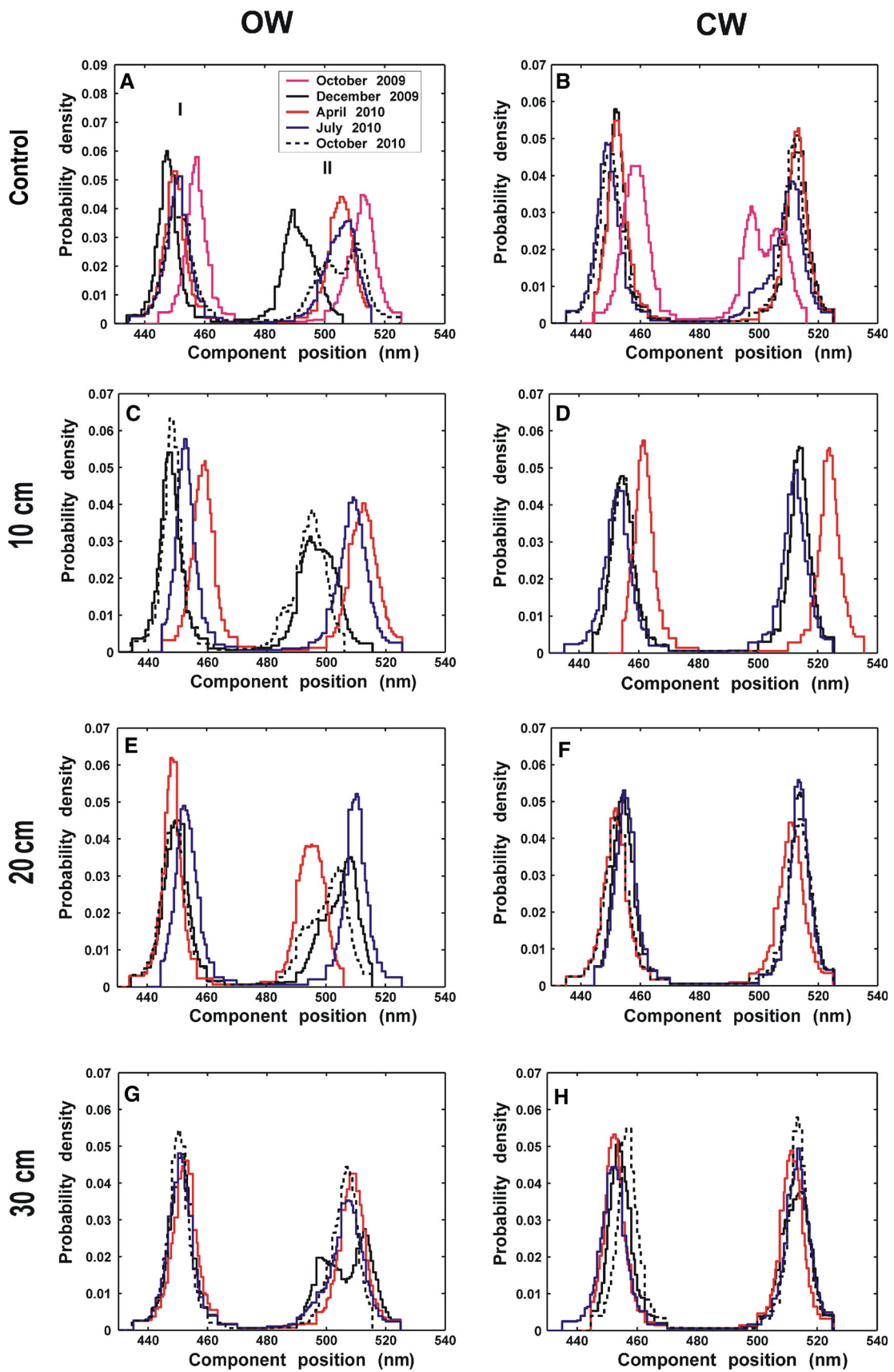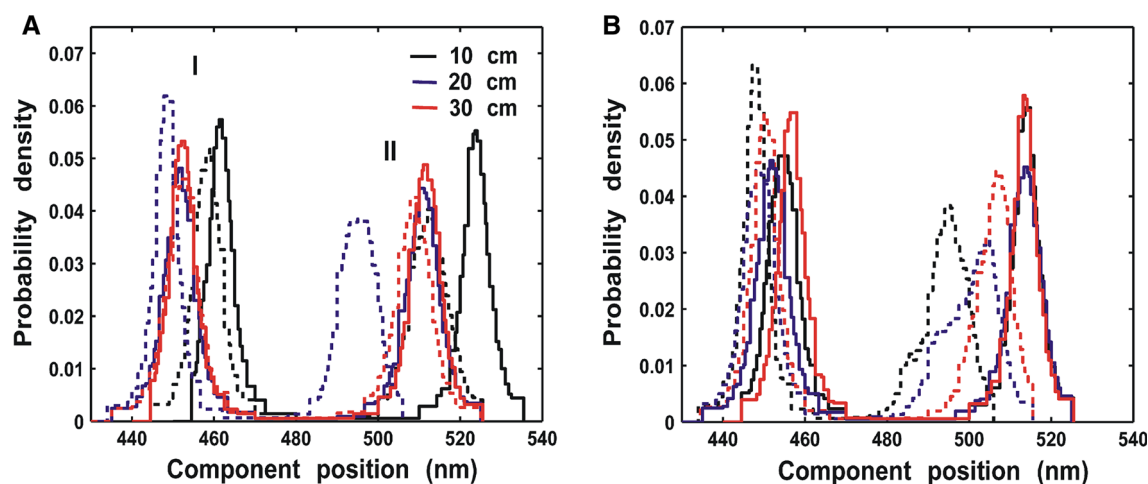
Fig. 8 APDs for opposite (*dashed lines*) and compression (*solid lines*) wood, in **a** the April (2010) and **b** the October (2010) samples of the mechanically treated trees; I, II: short-and long-APD wavelength components, respectively

for the red shift of the long-wavelength emission maxima in CW spectra compared to OW, the longer the conjugated polymeric structure, the higher the red shift of the corresponding emission maxima (Donaldson et al. 2010; Djikanovic et al. 2012). Such structures are proposed to increase mechanical rigidity of molecules by parallel packing of the long chains of alternating C=C/C–C bonds and by restriction of the rotation around the bonds (Donaldson et al. 2010). In this view, *P. omorika* trees may respond to bending by changing the size of the rigid chain structures of lignin although it is not clear what effect these molecular changes have on cell wall properties and how this might influence the gravitropic response.

Table 1 shows the shifts of corresponding APD component (I and II) positions between CW and OW in control plants, and in the three stem segments (at 10, 20 and 30 cm from stem base) of plants exposed to static bending. The matching graphs in Fig. 8, for the April (2010) and October (2010) samples, as an example, illustrate these APD components' shifts. The intention was to point to trends in spectral changes, related to molecular (lignin) differences, between CW and OW. As explained above, wavelength positions of resolved band components (marked as I–II, Table 1) are correlated with the length of the part of the macromolecular (lignin) chain that consists of conjugated bonds according to the Free-Electron Molecular Orbital (FEMO) method (Donaldson et al. 2010). In both control and treated plants, the long-wavelength component (II) for CW is red shifted relative to the corresponding component of OW (Table 1). The shifts clearly decrease from the base to the top of the stems in both April (2010) and October (2010) samples. In the April (2010) samples, the shift is lowest in the top segment. This indicates a more severe compression wood response (longer conjugated polymeric (lignin) domains making more rigid molecular structures) in segments at 10 and 20 cm from the

stem base compared to the top segment. In July 2010 (Fig. 7; Table 1), as an exception the shifts are similar for all three segments. The shifts of the short wavelength spectral component (component I, Table 1; Figs. 7, 8) in various samples are not so consistent. They reflect variations in the microenvironment composition and symmetry of the structures around the corresponding fluorophore(s) (Lakowicz 2006), as a relatively variable property.

Structural modifications of lignin may be related to the response to environmental conditions. The examples are both OW and CW APDs of the October 2009 samples of the control tree (Fig. 7a, b) and April 2010 base stem segment of the bent tree (Fig. 7c, d), in which the red-shifted position of the long-wavelength APD component (II) compared with the other samples (Fig. 7a, b, c, d) indicates formation of more rigid lignin structures in these seasons. In CW of bent trees, the indicators of cell wall structure change, such as fluorescence emission spectra, peak intensities and shifts in the positions of the long-wavelength spectral components, decreased from stem base to the top, in line with decrease in bending moment, whereas the CW amount increased (as a cumulative response to both static bending and stem overcorrection growth for achieving lean correction). This suggests that mechanical stress caused by static bending at the 90° angle is far more severe compared to the stress generated by achieving lean correction, and confirms that cell wall structures are more precise indicators of mechanical stress severity than the amount of CW formed.

Conclusions

Fluorescence microscopy including spectroscopy and deconvolution analysis show that the response to severe long-term bending stress in a slow-growing juvenile

conifer species results in a dramatic change in biomass distribution compared to control trees with very low amount of opposite wood relative to the large amount of compression wood formation. Assessment of cell wall structure and composition provides a more precise indicator of compression wood severity than the amount of compression wood formed. These cell wall characteristics show a correlation with the magnitude of applied stress related to distance from the point of bending.

References

Albinsson B, Li S, Lundquist K, Stomberg R (1999) The origin of lignin fluorescence. J Mol Struct 508:19–27

Altaner CM, Tokareva EN, Jarvis MC, Harris PJ (2010) Distribution of (1-4)-β-galactans, arabinogalactan proteins, xylans and (1-3)-β-glucans in tracheid cell walls of softwoods. Tree Physiol 30:782–793

Castellan A, Davidson RS (1994) Steady-state and dynamic fluorescence emission from *Abies* wood. J Photochem Photobiol A Chem 78:275–279

Djikanović D, Simonović J, Savić A, Ristić I, Bajuk-Bogdanović D, Kalauzi A, Cakić S, Budinski-Simendić J, Jeremić M, Radotić K (2012) Structural differences between lignin model polymers synthesized from various monomers. J Polym Environ 20:607–617

Donaldson LA (1992) Lignin distribution during late wood formation in *Pinus radiata* D. Don. IAWA Bull ns 13:381–387

Donaldson LA (2013) Softwood and hardwood lignin fluorescence spectra of wood cell walls in different mounting media. IAWA J 34:3–19

Donaldson LA, Knox JP (2012) Localisation of cell wall polysaccharides in normal and compression wood of radiata pine—relationships with lignification and microfibril orientation. Plant Physiol 158:642–653

Donaldson LA, Singh AP (2013) Structure and formation of compression wood. In: Fromm J (ed) Cellular aspects of wood formation, plant cell monographs. Springer, Berlin, pp 225–256

Donaldson LA, Grace JC, Downes G (2004) Within tree variation in anatomical properties of compression wood in radiata pine. IAWA J 25:253–271

Donaldson LA, Radotić K, Kalauzi A, Djikanović D, Jeremić M (2010) Quantification of compression wood severity in tracheids of *Pinus radiata* D. Don using confocal fluorescence imaging and spectral deconvolution. J Struct Biol 169:106–115

Downes GM, Moore GA, Turvey ND (1994) Variations in response to induced stem bending in seedlings od *Pinus radiata*. Trees 8:151–159

Falkehag SI, Marton J, Adler E (1966) Chromophores in Kraft lignin. Lignin structure and reactions. Adv Chem Ser 59:75–89

Fukushima K, Terashima N (1991) Heterogeneity in formation of lignin Part XV: formation and structure of lignin in compression wood of *Pinus thunbergii* studied by microautoradiography. Wood Sci Technol 25:371–381

Jones L, Seymour GB, Knox JP (1997) Localization of pectic galactan in tomato cell walls using a monoclonal antibody specific to (1,4)-β-D galactan. Plant Physiol 113:1405–1412

Kalauzi A, Mutavdžić D, Djikanović D, Radotić K, Jeremić M (2007) Application of asymmetric model in analysis of fluorescence spectra of biologically important molecules. J Fluoresc 17:319–329

Kern KA, Ewers FW, Telewski FW, Koehler L (2005) Mechanical perturbation affects conductivity, mechanical properties and aboveground biomass of hybrid poplars. Tree Physiol 25:1243–1251

Konschin H, Sundholm F (1974) Protolytic dissociation of electronically excited phenols related to lignin. II. Isoeugenol and coniferyl alcohol. Finn Chem Lett 1:46–49

Lachenbruch B, Johnson GR, Downes GM, Evans R (2010) Relationships of density, microfibril angle, and sound velocity with stiffness and strength in mature wood of Douglas-fir. Can J For Res 40:55–64

Lakowicz JR (2006) Principles of fluorescence spectroscopy, 3rd edn. Springer, NY, pp 97–155

Lundquist K, Josefsson B, Nyquist G (1978) Analysis of lignin products by fluorescence spectroscopy. Holzforschung 32:27–32

Nanayakkara B, Manley-Harris M, Suckling ID, Donaldson LA (2009) Quantitative chemical indicators to assess the gradation of compression wood. Holzforschung 63:431–439

Nanayakkara B, Lagane F, Hodgkiss P, Dibley M, Smaill S, Riddell M, Harrington J, Cown D (2014) Effects of induced drought and tilting on biomass allocation, wood properties, compression wood formation and chemical composition of young *Pinus radiata* genotypes (clones). Holzforschung 68:455–465

Olmstead JA, Gray DG (1997) Fluorescence spectroscopy of cellulose, lignin and mechanical pulps: a review. J Pulp Paper Sci 23:571–581

Radotić K, Kalauzi A, Đikanović D, Jeremić M, Leblanc RM, Cerović ZG (2006) Component analysis of the fluorescence spectra of a lignin model compound. J Photochem Photobiol B Biol 83:1–10

Sinott EW (1952) Reaction wood and the regulation of tree form. Am J Bot 39:69–78

Telewski FW, Jaffe MJ (1986) Thigmomorphogenesis: the role of ethylene in the response of *Pinus taeda* and *Abies fraseri* to mechanical perturbation. Physiol Plant 66:227–233

Telewski FW, Pruyn ML (1998) Thigmomorphogenesis: a dose response to flexing in *Ulmus americana* seedlings. Tree Physiol 18:65–68

Terashima N, Fukushima K (1988) Heterogenity in formation of lignin—XI: an autoradiographic study of the heterogeneous formation and structure of pine lignin. Wood Sci Technol 22:259–270

Timell TE (1986) Compression wood in gymnosperms, 1st edn. Springer, Heidelberg, pp 318–322